Magnetic Resonance Imaging 61 (2019) 239–246

Contents lists available at ScienceDirect

Magnetic Resonance Imaging

journal homepage: www.elsevier.com/locate/mri

Original contribution

In vivo ^{31}P-MRS of muscle bioenergetics in marine invertebrates: Future ocean limits scallops' performance

Christian Bock[a,*], Felizitas C. Wermter[a,b], Burgel Schalkhausser[a], Martin E. Blicher[c], Hans-O. Pörtner[a,b], Gisela Lannig[a], Mikael K. Sejr[d]

[a] Integrative Ecophysiology, Alfred Wegener Institute Helmholtz Centre for Polar and Marine Research, Am Handelshafen 12, 27570 Bremerhaven, Germany
[b] University of Bremen, Bibliothekstraße 1, 28359 Bremen, Germany
[c] Greenland Climate Research Centre, Greenland Institute of Natural Resources, Kivioq 2, 3900 Nuuk, Greenland
[d] Arctic Research Center, Aarhus University, Ny Munkegade byg 1540, 8000 Aarhus C, Denmark

ARTICLE INFO

Keywords:
Chemical shift imaging (CSI)
pH
Phosphagen
Energy metabolism
Aerobic power budget
Bivalves

ABSTRACT

Object: Dynamic *in vivo* ^{31}P-NMR spectroscopy in combination with Magnetic Resonance Imaging (MRI) was used to study muscle bioenergetics of boreal and Arctic scallops (*Pecten maximus* and *Chlamys islandica*) to test the hypothesis that future Ocean Warming and Acidification (OWA) will impair the performance of marine invertebrates.

Materials & methods: Experiments were conducted following the recommendations for studies of muscle bioenergetics in vertebrates. Animals were long-term incubated under different environmental conditions: controls at 0 °C for *C. islandica* and 15 °C for *P. maximus* under ambient PCO_2 of 0.039 kPa, a warm exposure with +5 °C (5 °C and 20 °C, respectively) under ambient PCO_2 (OW group), and a combined exposure to warmed acidified conditions (5 °C and 20 °C, 0.112 kPa PCO_2, OWA group). Scallops were placed in a 4.7 T MR animal scanner and the energetic status of the adductor muscle was determined under resting conditions using *in vivo* ^{31}P-NMR spectroscopy. The surplus oxidative flux (Q_{max}) was quantified by recording the recovery of arginine phosphate (PLA) directly after moderate swimming exercise of the scallops.

Results: Measurements led to reproducible results within each experimental group. Under projected future conditions resting PLA levels (PLA_{rest}) were reduced, indicating reduced energy reserves in warming exposed scallops *per se*. In comparison to vertebrate muscle tissue surplus Q_{max} of scallop muscle was about one order of magnitude lower. This can be explained by lower mitochondrial contents and capacities in invertebrate than vertebrate muscle tissue. Warm exposed scallops showed a slower recovery rate of PLA levels (k_{PLA}) and a reduced surplus Q_{max}. Elevated PCO_2 did not affected PLA recovery further.

Conclusion: Dynamic *in vivo* ^{31}P-NMR spectroscopy revealed constrained residual aerobic power budgets in boreal and Arctic scallops under projected ocean warming and acidification indicating that scallops are susceptible to future climate change. The observed reduction in muscular PLA_{rest} of scallops coping with a warmer and acidified ocean may be linked to an enhanced energy demand and reduced oxygen partial pressures (PO_2) in their body fluids. Delayed recovery from moderate swimming at elevated temperature is a result of reduced PLA_{rest} concentrations associated with a warm-induced reduction of a residual aerobic power budget.

1. Introduction

Anthropogenic CO_2 emissions are causing global warming and decreasing oceanic pH values, known as ocean warming and acidification (OWA) [1], with potentially severe consequences for marine life [2]. Depending on the climate model used, the global mean temperature is projected to rise by 2–3 °C while CO_2 concentrations will increase by up to 0.1 kPa PCO_2, accompanied by a drop in oceanic pH by up to 0.32 units until 2100 [3].

Ocean warming has a direct impact on all marine ectothermal organisms, whose body temperature changes with environmental temperature. Due to thermodynamic relations, known as the Q_{10} rule of van't Hoff, physiological/biochemical processes increase with increasing temperatures bearing consequences for organismal energy budget and aerobic performance [4,5]. Marine ectotherms are adapted to their environmental temperature regime implying that they are

* Corresponding author.
E-mail address: Christian.Bock@awi.de (C. Bock).

https://doi.org/10.1016/j.mri.2019.06.003
Received 19 February 2019; Received in revised form 15 May 2019; Accepted 2 June 2019

capable of fueling maintenance costs and allocating surplus energy towards growth, exercise and reproduction. Outside of the optimal thermal range temperature-induced impairment of the energy budget leads to decreased performance capacities and it is hypothesized that ocean acidification will exacerbate such warming-induced energetic disturbances [6].

Scallops are exceptional among bivalves since most species are active swimmers. Their swimming ability plays an important role in protection against predators [7] and in colonizing new habitats [8]. In combination with specific shell morphology swimming is realized/performed by the interplay of two muscle types: the smaller tonic or catch muscle and the main phasic adductor muscle. The phasic muscle consists of white muscle fibers from a fast-twitching type enabling swimming by jet propulsion *via* clapping [9]. Clapping is mainly fueled by the depletion of phosphagen stores which are hydrolyzed to replenish the ATP consumed during swimming. In contrast, the tonic muscle is an aerobic slow-twitching muscle type with relatively high mitochondrial content and is predominantly used for prolonged valve closures [9,10]. In contrast to blue mussels or oysters, scallops are usually not as tightly closed and thus can still rely on aerobic energy production during this time. Muscle use and bioenergetics in bivalves differ greatly from that in vertebrates and there is still limited knowledge of functional patterns and associated metabolism in molluscan muscles. One main difference is the use of arginine phosphate (PLA) *vs.* phosphocreatine (PCr) as a phosphagen source to buffer ATP levels during exercise [9,10]. In mollusks, during recovery from moderate muscle work, PLA in the phasic adductor muscle is re-synthesized by transphosphorylation from ATP produced by mitochondrial oxidative phosphorylation [9–11]. After exhaustive exercise re-phosphorylation of arginine is additionally supported by transphosphorylation from ATP, which is produced by anaerobic glycolysis forming the arginine derivate octopine [9,10,12].

In vivo ^{31}P-NMR spectroscopy enables the online measurement of the cellular energy status and metabolism, tracing the use and regeneration of high-energy phosphates ATP and phosphagen, such as PCr or PLA, and their end product, inorganic phosphate (Pi). Intracellular pH (pHi) can be determined from the position of the Pi signal within the NMR spectrum [13]. This approach has successfully been applied to scallops [14,15].

In 1997 Paganini and co-authors [16] introduced dynamic *in vivo* ^{31}P-NMR spectroscopy to determine the muscular maximum oxidative flux (Q_{max} [ATP μmol/g/min]) from the recovery rate of PCr, which was followed and analyzed from consecutive *in vivo* ^{31}P-NMR spectra after moderate exercise in rats. In fully aerobic muscle PCr is re-synthesized from ATP which is replenished by mitochondrial oxidative phosphorylation and the recovery rate of phosphagen thus mainly reflects the maximal phosphorylation capacity of operative muscle mitochondria. This approach was cross-validated by oxidative capacity measurements in mitochondria isolated from muscle biopsies [17]. Thus, in vertebrate muscle PCr displays a mono-exponential recovery rate under moderate exercise providing constant intracellular pH and unchanged magnesium concentrations [18]. Accordingly, following moderate exercise in bivalves, the mono-exponential recovery rate of PLA concentration reflects the maximum surplus oxidative flux of a molluscan muscle. Another technique that was frequently used in the past for measuring phosphagen turnover is saturation transfer ^{31}P-NMR spectroscopy. This technique was already used in an *in vitro* study to determine kinetic properties of arginine kinase and was published on isolated phasic muscle of a scallop [19]. Saturation transfer ^{31}P-NMR spectroscopy assesses oxidative muscle metabolism under resting condition and therefore reflect steady-state turnover and accordingly mitochondrial activity at rest and is therefore not the method of choice for exercise studies [20].

Guderley and Pörtner proposed a concept of a metabolic power budget for (active) marine ectotherms including scallops [4]. It suggests that all organism functions have specific aerobic costs fueled by a total aerobic power budget, which is constant and defines the organism's capacity to carry out all or some of them at a time as the available energy has to be divided between the different functions. The aerobic power budget thus determines the organism's steady state performance capacity for growth, locomotion, recovery of exercise or digestion and relies on the overall mitochondrial oxidative capacity. Towards the limits of an organism's environmental thermal range, the aerobic performance becomes constrained, as elaborated by the concept of oxygen and capacity limited thermal tolerance (OCLTT, [21]). If no temperature-dependent metabolic adjustments take place, the warming-induced rise in maintenance costs of ectotherms results in energetic trade-offs as the costs have to be fueled at the expense of other fitness-related parameters. Experimental study of this relationship ideally requires animals to undergo different steady state levels of performance (*e.g.* steady state swimming at different speeds in pelagic fish). However, many animals do not show such a steady state locomotion but use activity bouts only during attack or escape responses, that can be fueled by a mix of aerobic and anaerobic metabolism. Studying tradeoffs in aerobic energy budget involving different modes and levels of exercise are thus rather complicated. In scallops the restoration of PLA during recovery is an aerobic process [9], therefore we used two scallop species, the king scallop, *Pecten maximus*, and the Iceland scallop, *Chlamys islandica*, as animal models for such studies. Many bivalves including scallops show only partial or no compensation in standard metabolic rate to changing environmental temperatures [22–25]. We aim to link our earlier investigations of OWA impact on energy metabolism and swimming performance of scallops (see [25]) with a more in-depth study of the underlying muscle bioenergetics. Based on an established methodology for studying pHi and muscle bioenergetics by *in vivo* ^{31}P-NMR spectroscopy [15], we tested the applicability of dynamic ^{31}P-NMR spectroscopy. Scallops were long-term incubated at control, elevated temperature (+5 °C above the environmental summer mean) and increased PCO_2 levels (~0.112 kPa) as projected for the end of this century. We determined the energetic status of the adductor muscle using *in vivo* ^{31}P-NMR spectroscopy under resting conditions and after moderate exercise. The surplus maximum oxidative flux (Q_{max}) was estimated by measuring the recovery rate of PLA directly after the swimming trials. We interpret this flux to represent the surplus rate of aerobic energy production that is allocated to phosphagen repletion after other baseline costs may be met. According to the theory of the aerobic power budget [4] we hypothesize that the rising maintenance costs under ocean warming (OW) and OWA will cause constraints on the residual aerobic power budget of scallop muscle, with feedbacks on the animals' aerobic performance capacities.

2. Materials and methods

2.1. Animal incubation

For detailed information on the animals' set up of the long-term incubation facilities and incubation parameters see Schalkhausser et al. [25]. In brief, wild living king scallops, *Pecten maximus* (Linnaeus 1758) were purchased in September 2011 from the Marine Station Roscoff ("Station Biologique de Roscoff", at Morlaix Bay, France). At the time of collection, the ambient temperatures were around 11–14 °C. Wild Iceland scallops, *Chlamys islandica* (O. F. Müller, 1776) were collected in June 2011 at an ambient temperature of 0 °C using a triangulated dredge at 50–60 m in the outer Kobbefjorden, southwest Greenland. The annual temperature variation in Kobbefjorden in 30 m depth varies from −1.5 °C to 3 °C [26]. At the Alfred Wegener Institute (Bremerhaven, Germany) scallops were placed in recirculating aerated aquarium systems at salinity levels of 32–33 psu and 0 °C and 15 °C, respectively. Specimens taken from the aquarium system served as control group and were kept under present-day normocapnic conditions (PCO_2 level of ~0.039 kPa, 390 μatm) at 0 °C and 15 °C, respectively. To mimic future warming randomized groups of scallops were incubated

Table 1
Physicochemical conditions of seawater during the incubation under control, ocean warming (OW) and ocean warming and acidification (OWA) *C. islandica* (CI) and of *P. maximus* (PM).

Treatment PM	Control	OW	OWA
Temperature (°C)	15.0 ± 0.08	19.6 ± 0.3	19.8 ± 0.2
PCO_2 (kPa)	n.d.	0.045 ± 0.004	0.117 ± 0.024
pH (NBS scale)	8.03 ± 0.03	8.15 ± 0.03	7.86 ± 0.08

Treatment CI	Control	OW	OWA
Temperature (°C)	0.1 ± 0.4	5.0 ± 0.1	5.0 ± 0.4
PCO_2 (kPa)	0.034 ± 0.006	0.036 ± 0.009	0.114 ± 0.027
pH (NBS scale)	8.22 ± 0.08	8.21 ± 0.05	7.82 ± 0.16

for 50 days in temperature-control rooms in recirculation systems at 5 °C and 20 °C, respectively. The systems were continuously bubbled with a specific gas mixture to reach seawater PCO_2 values of either present-day of ~0.039 kPa (390 μatm, OW group) or values projected for 2100 of ~0.112 kPa (1120 μatm, OWA group). The water was exchanged at least twice a week. Water parameters in both, control and incubation systems were measured twice a week (see Table 1). Shell dimensions (height, length, width in [cm]) were measured using a caliper and did not differ prior to and after the incubation, irrespective of experimental group. To account for possible side effects due to size differences animals from similar size (shell length) were chosen, around 12 cm for *P. maximus* and 8 cm for *C. islandica*.

Animals were drip-fed live phytoplankton (SA Premium Reef Blend, *coralsands*) three times per week for at least 6 h. Dependent on acclimation temperature the concentrations varied between 0.6 and 1.1 × 10^6 cells h^{-1} g^{-1} bivalve biomass to account for different energetic demands and to prevent the possible impact of food limitation on high-energy phosphates. Indeed, incubation conditions did not lead to different condition indices in the scallops (9.0 ± 0.9 (0 °C), 9.3 ± 1.9 (5 °C) and 7.4 ± 0.7 (5 °C + CO_2) for *C. islandica*) and (13.6 ± 2.3 (10 °C), 13.0 ± 1.0 (20 °C), 11.7 ± 1.5 (20 °C + CO_2) for *P. maximum*) [25].

Prior to measurements animals were starved for at least 12–24 h (depending on species and respective temperature) to avoid interference of postprandial metabolism and feces excretion.

2.2. Experimental setup and MR measurements

2.2.1. Exercise protocol/design

The experimental set-up used for *in vivo* ^{31}P-NMR spectroscopy studies followed the principal design as described in detail for MR studies on marine organisms [27]. Briefly, the scallop was placed and fixed on a piece of Velcro in a tempered Perspex chamber, similar to [15], that was continuously perfused with seawater from a water reservoir maintained under the specific conditions of the different experimental groups (control, OW and OWA). Chamber temperature was monitored continuously using a fiber-optic sensor (Luxtron 504, Polytec, Germany) that was fixed into the Perspex chamber and was recorded on a computer *via* a PowerLab system (AD-Instruments, Australia). Prior to stimulating swimming, the specimens' optimal position and localization inside the MR scanner was determined using pilot scans in all three directions. In addition, *in vivo* ^{31}P-NMR spectra were recorded under resting conditions for potential individual or group specific differences in the energy status. Stimulation was performed outside of the MR scanner without disconnecting the chamber from the recirculating system to minimize the handling time till the actual start of the recordings during the recovery phase. An experimental protocol for moderate exercise of scallops was designed assuming approximately the half of claps performed during exhausted exercise until fatigue. *P. maximus* was stimulated to clap ~30 times compared to 50–70 claps determined for exhausted swimming [15], whereas in *C. islandica* moderate stimulation resulted in 5 to 15 claps compared to 20–40 claps until fatigue [28]. Following recent studies on scallops, all animals were stimulated to swim by (repeated) injection of tap water into the mantle cavity until the animal performed the desired number of claps associated with moderate exercise [25,29]. A maximum of around 5 mL tab water was used for the entire stimulation period for all animals, which is negligible in light of the total reservoir volume of approximately 30 L of seawater. The pump rate for seawater recirculation was at least 0.5 L/min, making the exchange rate high enough to prevent an accumulation of tap water inside the animal chamber. Therefore, potential side effects from salinity changes in the experimental chamber or inside the mantle cavity can be excluded. Directly after stimulation the chamber was placed back into the MR scanner and measurements of the PLA recovery rate started in < 2 min after the last clap.

2.2.2. MR imaging and spectroscopy

All studies were performed in a 4.7 T horizontal MR scanner with actively shielded gradient coils (Bruker Biospec 47/40 Avance III System, Bruker, Germany) and a bore of 40 cm. MR images and NMR spectroscopy were conducted using a 5 cm triple-tunable (^{1}H-^{31}P-^{13}C) surface coil. The surface coil was placed directly under the chamber nearest to the adductor muscle of the scallops, maximizing signal strength and localization. After adequate tuning of the surface coil, zero frequency settings and field homogeneity were optimized. Pilot scans were collected right before and after stimulation using a multi-slice gradient echo sequences in all three directions to ensure the optimal position of the surface coil relative to the adductor muscle (matrix 256*256, FOV 15*15 cm, slice thickness 2.64 mm, TR: 100 ms, TE: 3 ms, scan time 12 s). Frequency setting and shimming were automatically re-adjusted right after exercise. For the determination of muscle size and the calculation of adductor muscle volume, rapid acquisition with relaxation enhancement (RARE) images optimized for morphological MRI of marine organisms [15,30,31], were performed in coronal and sagittal direction (matrix 256*256, FOV 12*12 cm, slice thickness 1.5 mm, TR: 10000 ms, TE: 13.7 ms, rare factor of 12, scan time 3.5 min). *In vivo* non-localized ^{31}P-NMR spectra were acquired using parameters similar to Bailey et al. [15] (number of scans: ns = 256 and a repetition delay of 1 s resulting in an accumulation time of 4 min 26 s for each spectrum). In addition, to test for partial side effects of surrounding tissues, *in vivo* localized ^{31}P-NMR spectra were obtained in control animals of *P. maximus* only using an image-selected *in vivo* spectroscopy (ISIS) sequence [32]. The pulse scheme consisted of eight selective inversion pulses to define a voxel. Each inversion pulse lasted for 18.5 ms. 0.15 ms block-pulses were used for detection. A repetition time of 1 s and ns = 128–256 resulted in an acquisition time between 17 and 34 min. The voxel size was 36*30*30 mm. *In vivo* ^{31}P-chemical shift imaging (CSI) was also performed on *P. maximus* to get an overview of PLA distribution under resting conditions [33]. The field of view was 12*12 cm with 16 by 16 phase encoding steps. A repetition time of 1 s was used resulting in a total scan time of 7 h. Data were processed with a zero filling from 1024 to 2.048 points in the time domain and an exponential line broadening of 10. The PLA map expressed in percentage was produced applying a linear filter using the CSI tool within the operating software of the MR scanner (ParaVision 5.1, Bruker, Germany). The noise level was set to 20% in the PLA map.

2.2.3. Spectral analysis and metabolic calculations

A block of *in vivo* ^{31}P-NMR spectra was accumulated under control conditions. NMR spectra were considered as resting conditions when the signal areas of the PLA and Pi peaks did not reveal any changes. A second block of ^{31}P-NMR spectra was acquired directly after exercise until recovery of the scallops. Complete recovery was assumed when the PLA concentration had returned to at least 95% of the resting value. For the control group in *P. maximus*, one non-localized and four localized experiments were acquired. The direct comparison of PLA

concentrations calculated from non-localized and localized ^{31}P-NMR spectra led to same results and did not show significant differences between both techniques. Therefore, to benefit from the better time resolution, non-localized ^{31}P-NMR spectroscopy was used for the analyses of OW and OWA groups of *P. maximus* and for all groups of *C. islandica*.

All spectra were processed automatically using a user routine [34] and signals were assigned relative to the PLA signal which was set to 0 ppm. pHi was calculated from the pH-dependent shift of Pi relative to the PLA peak, which served as an internal standard. pHi values were calculated for the specific temperature using temperature compensated equations adapted from Kost [35] and pK values adjusted to ionic strength obtained from Pörtner et al. [36].

PLA_{rest} and Pi concentrations were used as a measure of muscle energetic status of scallops [14] under control conditions. Signal integrals were calculated relative to the area under the α-ATP/ADP signal. Concentrations were quantified to an assumed free ATP concentration at rest of 3.75 µmol/g wet muscle tissue according to the concentration determined in *Argopecten purpuratus* [37].

For a direct comparison of the PLA kinetics between groups, the ordinate values were normalized to PLA_{norm} = PLA/(PLA + Pi). The rate constant of PLA re-synthesis (k_{PLA} [1/min]) was determined by fitting a single mono-exponential curve to PLA_{norm} after Hallman et al. [37]:

$$PLA_{norm}(t) = (PLA_{rest} - PLA_{ex}) * (1 - e^{-k_{PLA}*t}) + PLA_{ex}$$

where t is time [min], PLA_{rest} and PLA_{ex} [µmol/g ww tissue] are the PLA concentration under resting conditions and at the end of exercise, respectively. The values for k_{PLA} [1/min] were taken directly from the curve fit. The maximum surplus oxidative flux (Q_{max} [ATP µmol/g ww tissue/min]) was determined as the product of k_{PLA} and PLA_{rest} [17].

2.3. Statistics

Data sets were analyzed using GraphPad Prism (Version 4.0a, GraphPad Software Inc.). Mono-exponential curves were fitted using the curve fitter within Prism. A one-way analysis of variance (ANOVA) in combination with Dunnett's multiple comparison test was used to test for significant differences between control and experimental groups. In addition, a post test for a linear trend across groups was performed. ANOVA in combination with a Newman-Keuls test was used to identify differences in morphological and muscle bioenergetic parameters between groups (p-value < 0.05). Data are given as means ± SD.

3. Results

Fig. 1 presents an anatomical coronal MR image of *P. maximus* under resting conditions. The heart and the main organs are located on the left side of the image near the valve of the shell. The circular adductor muscle is located in the upper center of the MR image. The contrast of the MR image distinguishes the two muscle types. The main phasic muscle type is located in the center, whereas the much denser looking crescent shaped tonic muscle is located in the upper right part of the adductor muscle. The bright lines crossing the muscle in the MR image result from hemolymph (blood) perfusion, despite the existence of a developed vascular system in the adductor muscle. The purple box around the adductor muscle is indicating the field of view used for the localized NMR spectroscopy trials. The calculated volume of the adductor muscle from RARE images in the three groups (control, OW and OWA) varied between 20 and 26 cm^3 of *P. maximus* and between 6 and 10 cm^3 of the smaller scallop *C. islandica* without significant differences between the species-specific groups (data not shown).

Fig. 2 shows an example of a chemical shift image of the PLA distribution under control conditions overlaid on the corresponding anatomical MR image of *P. maximus*. The PLA distribution fits reasonably well with the anatomical properties of the adductor muscle, indicating a good localization of ^{31}P-NMR spectra in the phasic part of the adductor muscle. The highest PLA concentration was found in the center of the phasic muscle independent of the position of the surface coil relative to the phasic muscle.

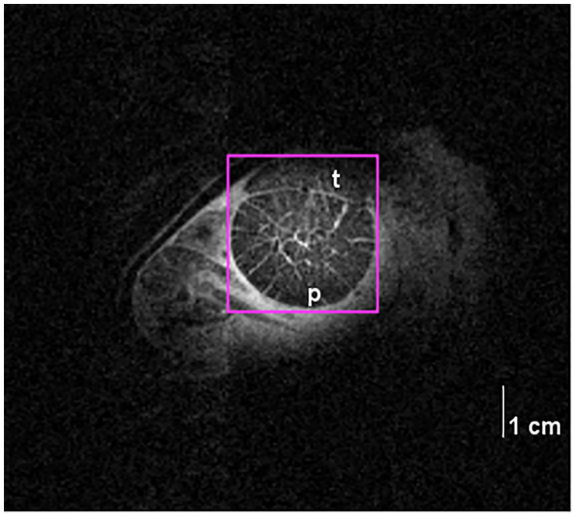

Fig. 1. Anatomical MRI of *P. maximus* showing the adductor muscle and its division in the phasic and tonic muscle types (p, t). Note the differences in hemolymph supply of the two muscle types. The purple box is marking the volume used for localized ^{31}P-NMR spectroscopy. (For interpretation of the references to color in this figure legend, the reader is referred to the web version of this article.)

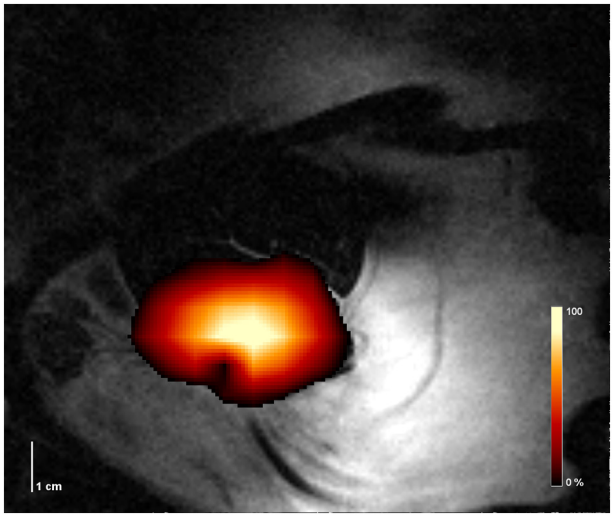

Fig. 2. Coronal view of a CSI overlaid on a corresponding anatomical MR image from *P. maximus*. The phasic muscle is located in the center of the image. Note, the excellent mapping of PLA concentration with the phasic muscle, indicating consistent localization.

Resting PLA concentrations from both species are presented in Fig. 3. PLA_{rest} was higher in *P. maximus* in comparison to *C. islandica* under control conditions. Between experimental groups PLA_{rest} was highest in the control group of both species and was significantly lower during warming (OW). In *P. maximus* resting PLA concentration was further decreased under the combined treatment (OWA). No significant changes in initial resting pHi values or ATP concentration were observed between the different groups in both species (data not shown).

All animals from both groups could be stimulated to swim by injection of tap water. At the start of the recovery phase individuals of *P. maximus* were usually slightly opened confirmed by pilot scans that were obtained for positioning before running *in vivo* ^{31}P-NMR spectra,

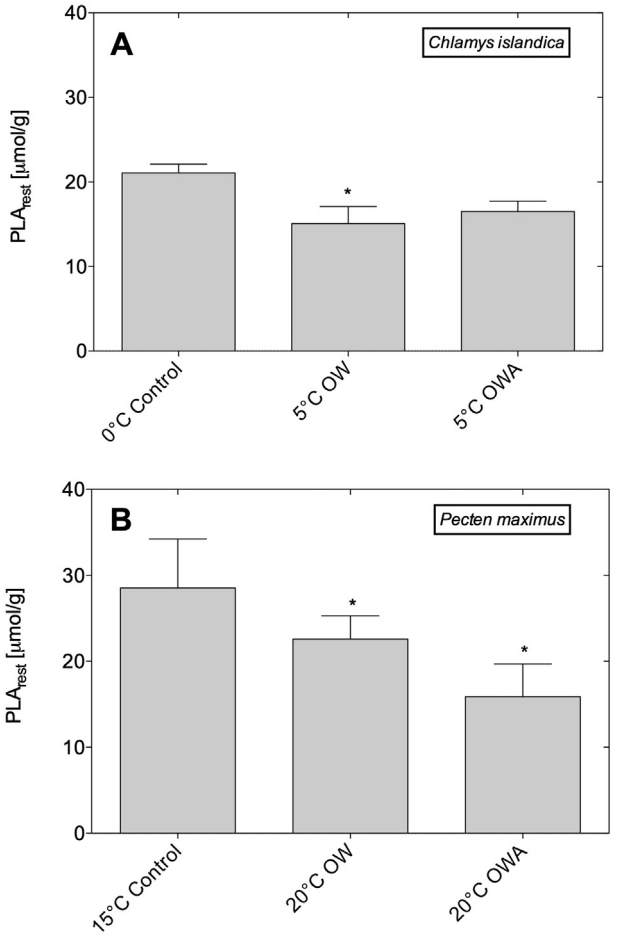

Fig. 3. Resting values of mean phospho-l-arginine (PLA_{rest}) concentrations determined in the adductor muscle of two scallop species under different environmental conditions, control, ocean warming (OW) and ocean warming & acidification (OWA). (A) *C. islandica* (control (n = 7), OW (*n* = 7) and OWA (n = 3)); (B) *P. maximus* (control (*n* = 3), OW (*n* = 5) and OWA (*n* = 4)). [PLA_{rest}] was highest in the control group for both scallop species. In *P. maximus* [PLA_{rest}] declined with a significant linear trend resulting in lowered concentrations in both experimental groups compared to control scallops. *Significantly different to data from the respective control group.

whereas some but not all individuals of the Arctic scallop *C. islandica* displayed a tight closure of the shells right after swimming performance.

Changes in metabolite signals during recovery after moderate exercise are shown in a typical stack plot of *in vivo* ^{31}P-NMR spectra for *P. maximus* (Fig. 4). Moderate swimming markedly increased the Pi and decreased the PLA signal. During the following recovery phase, PLA signal intensity increased immediately, accompanied by a decreasing Pi signal until steady state values were reached. In contrast, adenylate signals remained unchanged during the entire experimental protocol. No changes in the chemical shift of Pi signal could be observed within the resolution of the *in vivo* ^{31}P-NMR data indicating insignificant changes in pHi during recovery. Interestingly, individuals of *C. islandica*, that were tightly closed after swimming did not show any immediate PLA recovery. An increase of PLA rates was first observed when shells opened again (see Supplement 1).

Recovery rates of normalized PLA signals after moderate swimming under control and OW conditions are presented in Fig. 5 for both species. The recovery rates were best described by mono-exponential curves. Comparison between control and warming conditions clearly revealed a delayed recovery of PLA in both warm-exposed specimens. Additional exposure to ocean acidification had no further effect and OWA-exposed scallops displayed a similar delay in recovery rates as observed for the OW-exposed scallops (data not shown). Significant changes in pHi could not be observed during recovery in any of the experimental groups and species. Table 2 summarizes all determined variables from moderate swimming trails of all groups of both species including the results of the fit-analyses. The halftime of recovery ($t_{1/2}$) was about 10 min for *C. islandica* and about 18 min for *P. maximus* under control conditions. Interestingly, the halftime of recovery ($t_{1/2}$) was about 2 to 3 times longer under OW and OWA (26–27 min in *C. islandica*; and 37–55 min in *P. maximus*, respectively), leading to a similar delay in both species under these conditions. Accordingly, this led to smaller rate constants (k_{PLA}) and a reduced maximum surplus oxidative flux Q_{max}. However, due to the higher PLA_{rest} concentration the maximum surplus oxidative flux was higher in *P. maximus* compared to *C. islandica*.

4. Discussion

Our study confirms the applicability of dynamic *in vivo* ^{31}P-NMR spectroscopy to study muscle bioenergetics in a marine invertebrate by investigating two scallop species, *Pecten maximus* and *Chlamys islandica*. Since cytosolic acidification can inhibit mitochondrial respiration to different extents as shown for diverse vertebrate muscle types [18], heavy exercise can produce a long-lasting cytosolic acidification due to the accumulation of octopine during recovery in scallops [9]. However, we could easily stimulate both scallop species to swimming and observed no changes in muscle pHi values afterwards, indicating no acidosis that might constrain oxidative flux. A posterior acidification of pHi could be observed following fatigue exercise in our previous study, whereas a similar response as described here, was generated after a comparable (moderate) number of claps [15]. Therefore, a contribution of octopine formation and its degradation during the following recovery phase can be assumed as minimal and we conclude that the regeneration of PLA during recovery was attributed solely to the phosphorylation of arginine with ATP, that was produced by oxidative phosphorylation in accordance to [9].

4.1. Confirmation with biochemical data

Present resting PLA concentrations match literature data reported for scallops including *P. maximus* [15,37]. Since the concentrations were determined in relation to assumed ATP concentrations extracted from the literature [37], our data also validate the estimated absolute ATP concentrations (see Materials and methods section, [38]). The quality, *e.g.* line width and signal to noise ratio of the non-localized ^{31}P-NMR spectra as well as the pHi values, are also comparable to literature values [15,39]. Both ^{31}P-NMR modalities, localized and non-localized spectroscopy, reliably provided estimates of k_{PLA} and Q_{max} as measures of excess aerobic ATP generation in the adductor muscle of scallops.

4.2. Anatomical MRI and localization

The size of the adductor muscle determined from the MRI sets were similar between individuals of one species, but was species-dependent. The Iceland scallop, *C. islandica* had smaller muscle volumes than the king scallop, *P. maximus* which fits to the smaller size of *C. islandica*. From the anatomical MR images, the two types of the adductor muscle, tonic and phasic muscle, were clearly distinguishable. These specific morphological differences were also seen in MRIs of other bivalves, *e.g.* oysters [29]. Hemolymph-containing cavities that are displayed in the MR images indicate substantial differences in hemolymph supply between the two muscle types. In agreement with literature [39], the tonic muscle is supplied by a network of tiny cavities surrounding the muscle fiber packs, whereas the phasic muscle is only poorly vascularized by a few large lacunae. These morphological differences may indicate a better and more homogeneous hemolymph/oxygen supply to

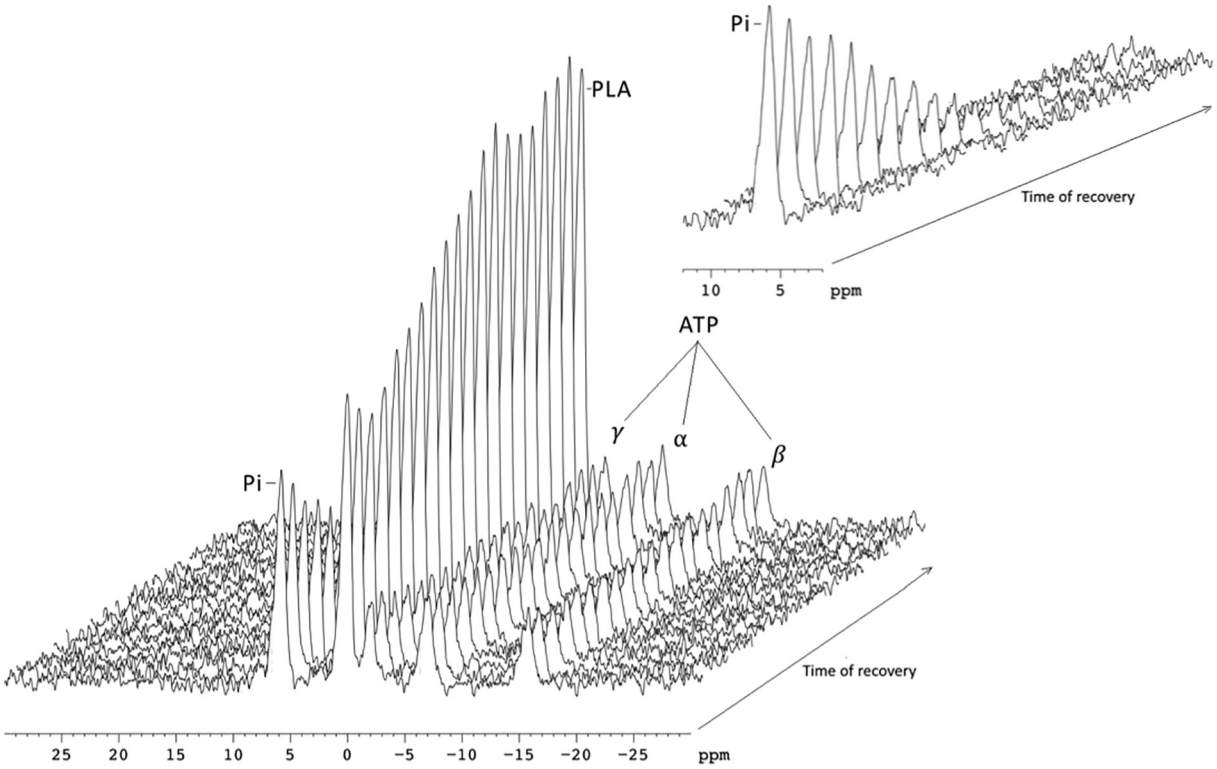

Fig. 4. Stack plot of *in vivo* ^{31}P-NMR spectra after moderate exercise of *P. maximus* under control conditions at 15 °C, showing the main high energy phosphates such as PLA and the three signals from ATP and the end product inorganic phosphate. After an initial increase of the inorganic phosphate (Pi) signal right after swimming a subsequent decrease of the signal accompanied by the recovery of the PLA signal is visible. See insert for a better visualization of the Pi signal. Changes in ATP signals did not occur (best visible for β-ATP at 16 ppm).

the more aerobic tonic muscle *versus* the more anaerobic operating phasic muscle supporting a more efficient and continuous energy supply [37].

The position and sensitive volume of the surface coil defines the volume of interest in dynamic ^{31}P NMR spectroscopy [40] and may result in partial volume effects. Our comparison of non-localized with localized ^{31}P-NMR spectroscopy in *P. maximus* revealed no or only a marginal contribution of the ^{31}P-NMR signals from surrounding tissues. This agrees with literature findings on PCr recovery rates determined in human calf muscle [40], where localized ^{31}P-NMR spectroscopy was compared with the use of surface coils. As reflected in the MRIs and the corresponding PLA map (Fig. 2) our careful consideration of the position and the diameter of the surface coil relative to the muscle volume ensured the recording of the relevant high energy phosphate signals from the adductor muscle. Furthermore, the determined concentrations of PLA rest are in the range of PLA rest values (22.46 ± 6.51 μmol/g wet muscle tissue) determined in the phasic muscle of the Bay scallop *Argopecten irradians* [20]. Despite of the relatively slow recovery rate of phosphagen in scallops compared to mammals the benefit of the much higher temporal resolution in non-localized than in localized dynamic ^{31}P-NMR spectroscopy is still of advantage and allows a more reliable determination of maximum oxidative flux from the mono-exponential fit.

4.3. Validation of the approach and comparison to mammalian studies

Creatine phosphate restores adenylate levels [41], and the relationship between the capacity of creatine kinase to rebuild ATP and PCr recovery rates was confirmed by Paganini et al. [16]. We applied this approach to the muscle bioenergetics of scallops, that poses arginine kinase instead of creatine kinase. Indeed, and without exception, the time slope of PLA recovery displayed the expected form of a mono-exponential slope, irrespective of the experimental group and the two species. Compared with mammalian studies the halftime of recovery ($t_{1/2}$) after moderate exercise was much slower resulting in a more than a magnitude lower k_{PLA} of 0.01–0.04 [1/min] *vs. e.g.* 0.5–1 [1/min] determined in mouse gastrocnemius muscle [16]. The differences are not surprising and can be explained by the different measurement temperatures (0/5 °C and 15/20 °C *vs.* 37 °C) and by the different rates of functioning and metabolism of the investigated tissue types. In contrast to terrestrial mammals the muscle of scallops operates in seawater and i) needs to overcome a much higher viscosity and ii) relies on a 30 times lower environmental oxygen content. Furthermore, scallops have an open circulatory system without respiratory pigments such as hemoglobin and their adductor muscle is only poorly perfused when compared to vertebrate muscles. Since maximal exercise performance depends on perfusion and thus oxygen provision [*e.g.* [41]] restricted oxygen supply to scallop muscle will consequently limit the organism's muscle performance as well as its ability to recover from exercise. In addition, mitochondrial enzyme capacities are much lower in muscle tissue of scallops than in vertebrates (fish) when performing at similar temperatures [42]. Taken together, this corroborates our findings of an order of magnitude lower maximum surplus oxidative flux in muscle tissue of a marine invertebrate.

4.4. Relation to climate-driven environmental changes

A recent comparison between various scallop species revealed a clear relationship between locomotor style and biochemical attributes of the adductor muscle showing PLA concentrations in relation to lifestyle activity, with highest PLA values at rest in very mobile scallops and lowest in a sessile species [38]. In the present study the dynamic ^{31}P-NMR spectroscopy approach was tested on two scallop species, the boreal scallop *P. maximus* from the Atlantic and the arctic scallop *C. islandica* from Greenland. Both species exhibit a similar moderate active swimming style in nature and levels of spontaneous activity during the

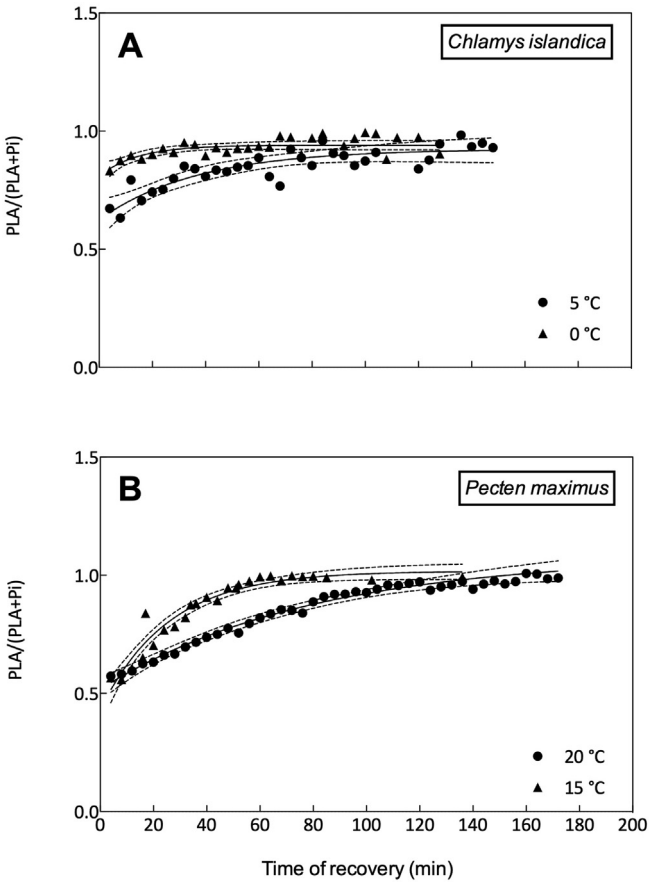

Fig. 5. Time course comparison of PLA recovery rates under control and OW conditions for (A) *C. islandica* and for (B) *P. maximus*. PLA is normalized as the ratio (PLA/(PLA + Pi)) for better comparison. The lines present the best fit from a mono exponential function. The dashed line presents the 95% confidence range from the fits. R^2 for the goodness of fit (*C.i*: 0.32 (0 °C); 0.25 (5 °C) and for *P.m*: 0.93 (15 °C); 0.75 (20 °C)). A clearly delayed recovery rate was observed under warming in comparison to control conditions in both species.

incubation periods were similar in all groups. Furthermore, the swimming performance of scallops is acclimated to their specific natural temperature regime as shown previously [15]. Therefore, the observed differences between species rely most likely on size differences of the muscle volume and resting PLA concentration rather than life style or differences of their natural habitat, such as temperature. The observed reduction in resting PLA levels of *P. maximus* and *C. islandica* under ocean warming (OW) and under the combination of ocean warming and acidification (OWA) was likely environmentally driven indicating that scallops experienced changes in energy status under OW and OWA.

In mammals phosphagen (PCr) levels are highest when ATP levels are high and free ADP levels low [43]. Low resting PCr concentrations led to an extended recovery period after exercise [44]. Furthermore, O_2 availability affects PCr recovery from submaximal exercise, in a way that under low oxygen availability recovery time was extended [45]. That this also holds true for PLA in scallops is supported by our observation in *C. islandica* that PLA recovery started not before the scallops opened the shell to improve oxygen availability and increase ventilation (see Supplementary figure).

In scallops PLA levels decrease with the number of claps and animals stop swimming when PLA levels reach a low limiting concentration in all investigated species [15]. An already lowered initial PLA_{rest} level thus suggests impaired performance. Indeed, time to fatigue was longer in *P. maximus* swimming under normocapnic conditions at 10 °C than at 20 °C [25]. In addition to an earlier exhaustion, the time to recover from exhaustive swimming was extended in the warmth [25], which matches the decelerated recovery rate of PLA levels (k_{PLA}) and reduced maximal surplus oxidative flux rates (Q_{max}) in the muscle of warm exposed scallops. Our previous findings of elevated energy demand and reduced hemolymph (blood) PO_2 of *P. maximus* under warming [see [25]] corroborate our line of thought that the PLA response is similar to the PCr response emphasizing the prominent role of oxygen availability for phosphagen recovery [45,46].

In line with the concept of the aerobic power budget [[4], see Introduction] the observed reduction in maximum surplus oxidative flux (Q_{max}) after long-term OW and OWA incubation is mainly a consequence of lowered hemolymph PO_2 which reduces the aerobic power budget, indicating that *P. maximus* and *C. islandica* reached thermal constraints already with potential consequences for growth [26]. Similar resting intracellular pH values in control, OW and OWA exposed scallops indicate compensation of the OA-induced extracellular acidosis at the intracellular level [25]. The associated rise in the costs of ion and acid-base regulation may cause the progressively reduced PLA_{rest} levels under OWA conditions, seen in *P. maximus* only and which were however not significantly different to PLA_{rest} levels under OW.

5. Conclusion

In conclusion, dynamic ^{31}P-NMR spectroscopy performed on scallops after moderate exercise provides further insights into the mechanisms underlying the limitations and effects of ocean warming and acidification on the bioenergetics of marine invertebrates. This approach is easily transferable to other research topics in comparative physiology which involve tissue energetics of mollusks such as in gastropods or cephalopods. Our results support the applicability of the aerobic power budget concept by Guderley & Pörtner [4]. In a future ocean, particularly given the ocean warming, invertebrates like scallops with an active life style and little capacity for thermal metabolic

Table 2
Summary of the results of the moderate swimming trials of *C. islandica* and *P. maximus*. PLA_{ex} values were extrapolated from the respective line fits.

Treatment	*Chlamys islandica*			*Pecten maximus*		
	0 °C		5 °C	15 °C		20 °C
	Control	OW	OWA	Control	OW	OWA
n	7	7	3	3	4	4
Claps	8 ± 3	9 ± 5	12 ± 7	33 ± 10	33 ± 12	30 ± 12
Pi/PLA_{ex}	0.21 ± 0.11	0.59 ± 0.32	0.79 ± 0.87	0.31 ± 0.30	0.78 ± 0.31	0.80 ± 0.49
PLA_{ex}	17.40	8.62	10.03	12.26	11.92	7.29
pHi_{rest}	7.51 ± 0.20	7.38 ± 0.06	7.27 (n = 2)	7.39 ± 0.09	7.46 ± 0.11	7.42 ± 0.06
pH_{iex}	7.46 ± 0.03	7.39 ± 0.04	7.55 ± 0.56	7.44 ± 0.04	7.41 ± 0.03	7.37 ± 0.05
k_{PLA} [1/min]	0.0698 ± 0.0285	0.0268 ± 0.0102	0.0254 ± 0.0074	0.0393 ± 0.0050	0.0127 ± 0.0027	0.0187 ± 0.0024
Q_{max} [mM ATP/min]	0.0114 ± 0.0027	0.0013 ± 0.0005	0.0020 ± 0.0008	0.0164 ± 0.0039	0.0078 ± 0.0004	0.0064 ± 0.0010
$t_{1/2}$ [min]	9.938	25.87	27.27	17.65	54.46	37.1

adjustments might be at risk. The climate-driven reduction in the residual aerobic power budget and the associated impairment of muscle bioenergetics might force scallops to a less active lifestyle making them more susceptible to predation. This might even be more pronounced if food availability is restricted.

Supplementary data to this article can be found online at https://doi.org/10.1016/j.mri.2019.06.003.

Acknowledgements

We like to thank Anette Tillmann for help with animal maintenance and Rolf Wittig for his help with processing the ^{31}P-NMR data. This project was supported by the AWI PACES2 program and is a contribution to the BMBF-funded project “Biological Impacts of Ocean Acidification” (BIOACID, FKZ 03F0608B).

References

[1] Pörtner HO. Ecosystem effects of ocean acidification in times of ocean warming: a physiologists view. Mar Ecol Prog Ser 2008;373:203–17.
[2] Seebacher F, White CR, Franklin CE. Physiological plasticity increases resilience of ectothermic animals to climate change. Nat Clim Change 2015;5:61–6.
[3] Contribution of working groups I, II and III to the fifth assessment report of the intergovernmental panel on climate change. In: Pachauri RK, Meyer LA, editors. IPCC climate change 2014: synthesis report. Geneva, Switzerland: IPCC; 2014. p. 151.
[4] Guderley HE, Pörtner HO. Metabolic power budgeting and adaptive strategies in zoology: examples from scallops and fish. Can J Zool 2010;88:753–63.
[5] Sokolova IM, Frederich M, Bagwe R, Lannig G, Sukhotin AA. Energy homeostasis as an integrative tool for assessing limits of environmental stress tolerance in aquatic invertebrates. Mar Environ Res 2012;79:1–15.
[6] Pörtner HO, Farrell AP. Ecology. Physiology and climate change. Science 2008;322:690–2.
[7] Brand AR. Chapter 12 scallop ecology: distributions and behavior. Developments in Aquaculture and Fisheries Science 2006;35:651–744.
[8] Scallop cultivation in the UK: a guide to site selection. http://www.cefas.defra.gov.uk/publications/files/scallop_cultivation.pdf; 2014, Accessed date: 21 August 2014.
[9] Livingstone DR, de Zwaan A, Thompson RJ. Aerobic metabolism, octopine production and phosphorarginine as sources of energy in the phasic and catch adductor muscles of the giant scallop *Placopecten magellanicus* during swimming and the subsequent recovery period. Comp Biochem Physiol B 1981;70:35–44.
[10] Grieshaber MK. Breakdown and formation of high-energy phosphates and octopine in the adductor muscle of the scallop, *Chlamys opercularis* (L.), during escape swimming and recovery. J Comp Physiol B 1978;126:269–76.
[11] Guderley HE, Rojas FM, Nusetti OA. Metabolic specialization of mitochondria from scallop phasic muscles. Mar Biol 1995;122:409–16.
[12] Moore E, Wilson DW. Nitrogenous extractives of scallop muscle: I. The isolation and a study of the structure of octopine. J Biol Chem 1937;119:573–84.
[13] Moon RB, Richards JH. Determination of intracellular pH by ^{31}P magnetic resonance. J Biol Chem 1973;248:7276–8.
[14] Jackson AE, de Freitas ASW, Hooper L, Mallet A, Walter JA. Phosphorus metabolism monitored by ^{31}P-NMR in juvenile sea scallop (*Placopecten magellanicus*) overwintering in pearl nets at a Nova Scotian aquaculture site. Can J Fish Aquat Sci 1994;51:2105–14.
[15] Bailey DM, Peck LS, Bock C, Pörtner HO. High-energy phosphate metabolism during exercise and recovery in temperate and Antarctic scallops: an *in vivo* ^{31}P-NMR study. Physiol Biochem Zool 2003;76:622–33.
[16] Paganini AT, Foley JM, Meyer RA. Linear dependence of muscle phosphocreatine kinetics on oxidative capacity. Am J Physiol 1997;272:C501–10.
[17] Lanza IR, Bhagra S, Nair KS, Port JD. Measurement of human skeletal muscle oxidative capacity by ^{31}P-MR spectroscopy: a cross-validation with *in vitro* measurements. J Magn Reson Imaging 2011;34:1143–50.
[18] Layec G, Malucelli E, Le Fur Y, Manners D, Yashiro K, Testa C, et al. Effects of exercise-induced intracellular acidosis on the phosphocreatine recovery kinetics: a ^{31}P MRS study in three muscle groups in humans. NMR Biomed 2013;26:1403–11.
[19] Graham RA, Ellington WR, Chih CP. A saturation transfer phosphorus nuclear magnetic resonance study of arginine phosphokinase in the muscle of marine mollusc. Biochim Biophys Acta 1986;887:157–63.
[20] Schmid AI, Schrauwen-Hinderling VB, Andreas M, Wolzt M, Moser E, Roden M. Comparison of measuring energy metabolism by different ^{31}P-magnetic-resonance techniques in resting, ischemic, and exercising muscle. Magn Reson Med 2012;67:898–905.
[21] Pörtner HO. Climate change and temperature-dependent biogeography: oxygen limitation of thermal tolerance in animals. Naturwissenschaften 2001;88:137–46.
[22] Pilditch CA, Grant J. Effect of temperature fluctuations and food supply on the growth and metabolism of juvenile sea scallops (Placopecten magellanicus). Mar Biol 1999;134:235–48.
[23] Peck LS, Pörtner HO, Hardewig I. Metabolic demand, oxygen supply, and critical temperatures in the Antarctic bivalve *Laternula elliptica*. Physiol Biochem Zool 2002;75:123–33.
[24] Lannig G, Flores JF, Sokolova IM. Temperature-dependent stress response in oysters, *Crassostrea virginica*: pollution reduces temperature tolerance in oysters. Aquat Toxicol 2006;79:278–87.
[25] Schalkhausser B, Bock C, Pörtner HO, Lannig G. Escape performance of temperate king scallop, *Pecten maximus* under ocean warming and acidification. Mar Biol 2014;161:2819–29.
[26] Blicher ME, Rysgaard S, Sejr MK. Seasonal growth variation in *Chlamys islandica* (Bivalvia) from sub-Arctic Greenland is linked to food availability and temperature. Mar Ecol Prog Ser 2010;407:71–86.
[27] Bock C, Satoris FJ, Pörtner HO. *In vivo* MR spectroscopy and MR imaging on non-anaesthetized marine fish: techniques and first results. J Magn Reson Imaging 2002;20:165–72.
[28] Schalkhausser B. Physiological effects of ocean warming and acidification on pectinid bivalves PhD Thesis Bremen: University of Bremen; 2015.
[29] Schalkhausser B, Bock C, Stemmer K, Brey T, Pörtner HO, Lannig G. Impact of ocean acidification on escape performance of the king scallop, *Pecten maximus*, from Norway. Mar Biol 2013;160:1995–2006.
[30] Lannig G, Cherkasov AS, Pörtner H O, Bock C, Sokolova IM. Cadmium-dependent oxygen limitation affects temperature tolerance in eastern oysters (*Crassostrea virginica Gmelin*). Am J Physiol Regul Integr Comp Physiol 20008; 294:R1338-R1346.
[31] Ziegler A, Knuth M, Mueller S, Bock C, Pohmann R, Schröder L, et al. Application of magnetic resonance imaging in zoology. Zoomorphology 2011;130:227–54.
[32] Ordidge RJ, Connelly A, Lohman JAB. Image-selected *in vivo* spectroscopy (ISIS). A new technique for spatially selective nmr spectroscopy. J Magn Reson 1969;66:283–94.
[33] Guilfoyle DN, Mansfield P. Chemical-shift imaging. Magn Reson Med 1985;2:479–89.
[34] Bock C, Sartoris FJ, Wittig RM, Pörtner HO. Temperature dependent pH regulation in stenothermal Antarctic and eurythermal temperate eelpout (*Zoarcidae*): an *in vivo* NMR study. Polar Biol 2001;24:869–74.
[35] Kost GJ. pH standardization for phosphorus-31 magnetic resonance heart spectroscopy at different temperatures. Magn Reson Med 1990;14:496–506.
[36] Pörtner HO, Bock C, Reibschläger A. Modulation of the cost of pHi regulation during metabolic depression: a ^{31}P-NMR study in invertebrate (*Sipunculus nudus*) isolated muscle. J Exp Biol 2000;203:2417–28.
[37] Pérez HM, Brokordt KB, Martínez G, Guderley HE. Locomotion versus spawning: escape responses during and after spawning in the scallop *Argopecten purpuratus*. Mar Biol 2009;156:1585–93.
[38] Tremblay I, Guderley HE. Scallops show that muscle metabolic capacities reflect locomotor style and morphology. Physiol Biochem Zool 2014;87:231–44.
[39] Hallman TM, Rojas-Vargas AC, Jones DR, Richards JG. Differential recovery from exercise and hypoxia exposure measured using ^{31}P- and ^{1}H-NMR in white muscle of the common carp *Cyprinus carpio*. J Exp Biol 2008;211:3237–48.
[40] Meyerspeer M, Robinson S, Nabuurs CI, Scheenen T, Schoisengeier A, Unger E, et al. Comparing localized and nonlocalized dynamic ^{31}P magnetic resonance spectroscopy in exercising muscle at 7T. Magn Reson Med 2012;68:1713–23.
[41] Meyer RA. Linear dependence of muscle phosphocreatine kinetics on total creatine content. Am J Physiol 1989;257:C1149–57.
[42] Guderley HE. Locomotor performance and muscle metabolic capacities: impact of temperature and energetic status. Comp Biochem Physiol B Biochem Mol Biol 2004;139:371–82.
[43] Smith RN, Agharkar AS, Gonzales EB. A review of creatine supplementation in age-related diseases: more than a supplement for athletes. F1000Research 2014;3:222.
[44] Francescato MP, Cettolo V, di Prampero PE. Influence of phosphagen concentration on phosphocreatine breakdown kinetics. Data from human gastrocnemius muscle. J Appl Physiol (1985) 2008;105:158–64.
[45] Haseler LJ, Hogan MC, Richardson RS. Skeletal muscle phosphocreatine recovery in exercise-trained humans is dependent on O_2 availability. J Appl Physiol 1999;86:2013–8.
[46] Lannig G, Storch D, Pörtner HO. Aerobic mitochondrial capacities in Antarctic and temperate eelpout (*Zoarcidae*) subjected to warm versus cold acclimation. Polar Biol 2005;28:575–84.